APPLIED AND ENVIRONMENTAL MICROBIOLOGY, Oct. 1988, p. 2556–2565
0099-2240/88/102556-10$02.00/0

Vol. 54, No. 10

Pyrene Degradation by a *Mycobacterium* sp.: Identification of Ring Oxidation and Ring Fission Products

MICHAEL A. HEITKAMP,† JAMES P. FREEMAN, DWIGHT W. MILLER, AND CARL E. CERNIGLIA*

National Center for Toxicological Research, Food and Drug Administration, Jefferson, Arkansas 72079

Received 19 April 1988/Accepted 19 July 1988

The degradation of pyrene, a polycyclic aromatic hydrocarbon containing four aromatic rings, by pure cultures of a *Mycobacterium* sp. was studied. Over 60% of [^{14}C]pyrene was mineralized to CO_2 after 96 h of incubation at 24°C. High-pressure liquid chromatography analyses showed the presence of one major and at least six other metabolites that accounted for 95% of the total organic-extractable ^{14}C-labeled residues. Analyses by UV, infrared, mass, and nuclear magnetic resonance spectrometry and gas chromatography identified both pyrene *cis*- and *trans*-4,5-dihydrodiols and pyrenol as initial microbial ring-oxidation products of pyrene. The major metabolite, 4-phenanthroic acid, and 4-hydroxyperinaphthenone and cinnamic and phthalic acids were identified as ring fission products. $^{18}O_2$ studies showed that the formation of *cis*- and *trans*-4,5-dihydrodiols were catalyzed by dioxygenase and monooxygenase enzymes, respectively. This is the first report of the chemical pathway for the microbial catabolism of pyrene.

Microbial degradation is a major factor affecting the persistence of polycyclic aromatic hydrocarbons (PAHs) in the environment. The ability of bacteria in water, soil, or sediment to degrade PAHs depends on the complexity of the PAH chemical structure and the extent of enzymatic adaptation by indigenous bacteria in response to chronic exposure to aromatic hydrocarbons (3, 10; C. E. Cerniglia and M. A. Heitkamp, *in* U. Varanasi, ed., *Metabolism of Polycyclic Aromatic Hydrocarbons in the Aquatic Environment*, in press). In general, PAHs containing two or three aromatic rings are readily degradable. Several bacteria have been isolated which are able to utilize these lower-molecular-weight PAHs as sole sources of carbon and energy (reviewed by Cerniglia and Heitkamp [in press]). However, PAHs containing four or more aromatic rings are recalcitrant and often genotoxic (23). To date, no bacteria have been reported which are able to utilize higher-molecular-weight PAHs as sole sources of carbon and energy. However, in a recent study and in the accompanying paper, we reported the isolation of a novel *Mycobacterium* sp. that can mineralize several unsubstituted, nitrated, and methylated PAHs containing four aromatic rings when cultured in growth medium containing organic nutrients (14, 15).

Metabolism plays an important role in both the bioactivation and detoxification of PAHs. It is known that carcinogenic PAHs are transformed to their ultimate genotoxic forms by monooxygenase enzyme systems in mammals (22). Alternatively, eucaryotic metabolism of PAHs may also produce ring-oxidation products that are not genotoxic and undergo further metabolism to conjugated detoxification products (4). The identity, enzymatic mechanisms, genetic control, and genotoxicity of carcinogenic ring oxidation products have been extensively studied in mammals and eucaryotic organisms (3, 10; Cerniglia and Heitkamp, in press).

Although chemical pathways and enzymatic mechanisms for the microbial metabolism of PAHs containing two or three aromatic rings have been well studied, investigations on the degradation of high-molecular-weight PAHs are scarce (9). Procaryotic metabolism of PAHs is believed to result solely in degradation and detoxification (Cerniglia and Heitkamp, in press).

We reported in the accompanying paper (15) on the isolation of a PAH-degrading *Mycobacterium* sp. In this study, we report on the use of the *Mycobacterium* sp. to determine the rate of degradation for the microbial metabolism of pyrene, a four-ringed PAH which is one of 16 PAHs on the list of priority pollutants compiled by the U.S. Environmental Protection Agency (21). In addition, the isolation and identification of ring oxidation and ring fission products as well as the enzymatic mechanisms involved in the initial ring oxidation reactions are reported.

MATERIALS AND METHODS

Chemicals. [4,5,9,10-^{14}C]pyrene with a specific activity of 59.5 mCi/mm was purchased from Chemsyn Science Laboratories, Lenexa, Kans. Pyrene was purchased from Chemical Service, Media, Pa. Chemical analyses of pyrene by gas chromatography-mass spectrometry (GC-MS) and high-pressure liquid chromatography (HPLC) showed that purity exceeded 99%. Bacterial growth media were purchased from Difco Laboratories, Detroit, Mich. Authentic *cis*-4,5-dihydroxy-4,5-dihydropyrene (pyrene *cis*-4,5-dihydrodiol) and *trans*-4,5-dihydroxy-4,5-dihydropyrene (pyrene *trans*-4,5-dihydrodiol) were supplied by Fred Beland, and authentic 1-hydroxypyrene was supplied by Peter Fu at the National Center for Toxicological Research.

Growth and exposure of *Mycobacterium* cultures to pyrene. *Mycobacterium* cultures were grown at 24°C in continuously mixed 125-, 500-, or 2,000-ml Erlenmeyer flasks containing 50, 300, or 1,200 ml of minimal basal salts (MBS) medium (15), respectively, supplemented with low levels (250 μg/liter) of peptone, yeast extract, and soluble starch. Starter cultures (125 ml) were inoculated with *Mycobacterium* colonies from MBS agar plates and grown for 96 h at 24°C (transferred twice) in MBS medium supplemented with nutrients and pyrene. The purity of starter cultures was determined by Gram staining and replating onto pyrene-coated MBS agar plates (14). Log-phase *Mycobacterium* cultures (1.5×10^6 cells per ml) were used to inoculate 300 ml of supplemented MBS medium containing 0.92 μCi of

* Corresponding author.
† Present address: Monsanto Co., St. Louis, MO 63167.

[4,5,9,10-^{14}C]pyrene and 0.5 μg of pyrene per ml and incubated in the dark at 24°C with shaking at 150 rpm. Experiments to determine the kinetics of pyrene metabolism by the *Mycobacterium* sp. were conducted with replicate 50-ml cultures which were extracted after 0, 3, 6, 18, 24, 48, 72, and 96 h of incubation.

Mycobacterium cultures for $^{18}O_2$ experiments were grown in 125-ml Erlenmeyer flasks capped with rubber septa. These cultures were grown for 48 h in an $^{18}O_2$ atmosphere at 24°C after exposure to 0.5 μg of pyrene per ml. The air space of these cultures was evacuated and overlaid with argon four times before the addition of 1 atm (ca. 101.25 kPa) of $^{18}O_2$ (99.8 atom%; Mound Facility, Miamisburg, Ohio). The relative concentrations of $^{16}O_2$ and $^{18}O_2$ in the flasks were determined by MS analyses of the headspace to be 96.8% $^{18}O_2$ at the beginning and 95.5% $^{18}O_2$ at the end of the experiment.

Analysis and identification of pyrene metabolites. Bacterial cells and culture medium were extracted with six equal volumes of ethyl acetate. The extracts were pooled, dried with anhydrous Na_2SO_4, and evaporated in vacuo at 40°C to 10 ml. The extracts were transferred to calibrated glass vials and evaporated to dryness under a gentle stream of dry argon. To enhance the recovery of acidic metabolites, the culture medium was acidified to pH 4.0 with 0.1 N HCl and extracted with 3 equal volumes of ethyl acetate.

Pyrene metabolites were isolated and purified by thin-layer chromatography (TLC) and HPLC. TLC analyses were performed with 500 μM silica gel GF plates (Analtech, Newark, Del.), and separation was achieved with either a benzene-hexane (1:1, vol/vol), hexane-acetone (8:2, vol/vol), or benzene-acetone-acetic acid (85:15:5, vol/vol/vol) solvent system.

The benzene-hexane solvent system was used to separate undegraded pyrene and other highly nonpolar biogenic chemicals from more polar pyrene metabolites. The hexane-acetone solvent system was used to elute ring oxidation products up the TLC plate, and the benzene-hexane-acetic acid system was used to separate the highly polar, possibly acidic, ring fission metabolites of pyrene that remained at or near the origin of the TLC plate with the first two solvent systems.

Reversed-phase HPLC analyses were performed as previously described (16), and separation was achieved with a methanol-water linear gradient solvent system (50 to 95% [vol/vol] methanol in 30 min) or with a methanol-water (55:45, vol/vol) isocratic solvent system. Repeated injections of ethyl acetate extracts on reversed-phase HPLC with subsequent collection of metabolite peaks resulted in the accumulation of small amounts of purified metabolites. These were used as metabolite standards for preparatory TLC (prep-TLC) enrichment of metabolites in crude extracts from large-scale, batch experiments. Enriched metabolite fractions from prep-TLC were further purified by repeated injections onto reversed-phase HPLC with the isocratic solvent system.

Direct probe MS and capillary column GC-MS analyses were performed as previously described (16). Metabolites were also derivatized by methylation or acetylation (18).

The UV-visible absorption spectra of pyrene metabolites were determined in methanol on a Beckman model DU-7 spectrophotometer (Beckman Instruments, Berkeley, Calif.). Infrared (IR) spectra of pyrene metabolites were determined on a Nicolet model MX-1 FT-IR spectrometer (Nicolet Instrument Corp., Madison, Wis.).

A Finnigan Instruments model 1015 mass spectrometer (Finnigan-MAT, San Jose, Calif.) equipped with a quadrupole mass filter and a Granville-Phillips (Boulder, Colo.) model 203 variable leak valve for gas introduction was used for headspace gas analyses of cultures incubated with $^{18}O_2$. Spectra were obtained at 70 eV over a scan range of 10 to 100 daltons.

Circular dichroism spectra were determined in methanol in a quartz cell of 1-cm path length at room temperature on a Jasco model 500A spectropolarimeter equipped with a Jasco DP-500 data processor.

The ^{1}H nuclear magnetic resonance (NMR) spectra were recorded on a Bruker WM500 spectrometer in either acetone-d_6, D_2O, or methylene chloride-d_2. The data were acquired under the following conditions: data points, 32,000; sweep width, 7,042 Hz; filter width, 17,800 Hz; temperature, 305 K; flip angle, 68°. The chemical shifts are reported in parts per million downfield from the internal standard tetramethylsilane. Assignments were made via homonuclear decoupling experiments and by consideration of substituent effects.

TABLE 1. Kinetic analysis of pyrene metabolism by a *Mycobacterium* sp.

Incubation time (h)	Total % mineralized	% of metabolites[a]						
		Polar	I	II	III	IV	V	Pyrene
3	1.5	0.3	0.2	0.4	0.4	0.5	0.7	97.5
6	5.0	0.2	0.3	0.7	1.1	0.5	0.3	96.9
18	29.2	0.4	1.0	3.4	0.9	0.6	0.4	93.3
24	39.6	0.4	1.0	5.1	1.0	0.5	0.2	91.8
48	47.3	1.9	2.1	62.8	3.3	0.9	2.0	27.0
72	48.8	4.6	5.5	77.3	3.6	1.7	1.0	6.3
96	52.4	4.5	1.5	83.2	3.6	1.2	0.9	5.1

[a] Values are presented as percentages of the organic-extractable ^{14}C-labeled residue. Metabolites and HPLC elution times were as follows: Polar, 2.5 to 3.5 min; I, 4.0 to 6.5 min; II, 7 to 10 min; III, 15 to 19 min; IV, 21.5 to 23.5 min; V, 25.5 to 27.5 min; pyrene, 33.5 to 36 min.

RESULTS

Kinetics of pyrene degradation and metabolite formation. The degradation of pyrene and the occurrence of metabolites were examined in an initial experiment in which *Mycobacterium* cultures and sterile controls were exposed to [^{14}C]pyrene and unlabeled pyrene for 96 h, respectively. After 48 to 96 h of incubation, 47.3 to 52.4% of pyrene was mineralized to CO_2 by the *Mycobacterium* sp. (Table 1). Figure 1 shows the UV and radioactivity HPLC elution profile for organic extracts from sterile control flasks and *Mycobacterium* cultures exposed to pyrene for 96 h. Pyrene had an HPLC retention time of 34.5 min (Fig. 1A). Abiotic degradation of pyrene did not occur in sterile control flasks. However, after 96 h of incubation most of the pyrene was degraded to metabolites by the bacterial cultures (Fig. 1B). Five metabolites of pyrene, designated I, II, III, IV, and V, were detected which had HPLC retention times of 5.2, 7.5, 16.6, 22.0, and 26.0 min, respectively. Highly polar residues, unretained on reversed-phase HPLC, eluted between 2.5 and 3.5 min. The HPLC peak observed at 35.0 min was undegraded pyrene.

A kinetics experiment was conducted to determine the time course for pyrene degradation and formation of specific metabolites by *Mycobacterium* cultures (Table 1). Over 40% of the pyrene was mineralized to CO_2 during the first 72 h of incubation. Although total organic-extractable residues dropped throughout the experiment because of mineraliza-

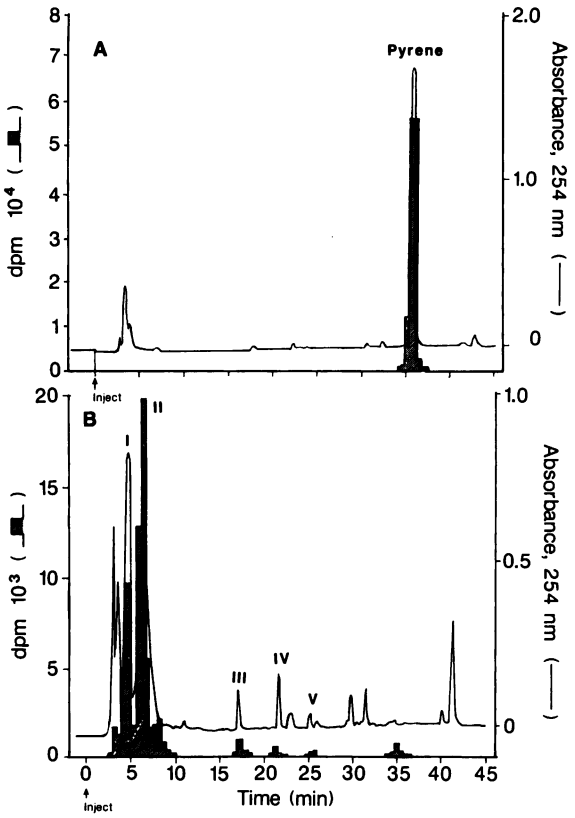

FIG. 1. HPLC elution profile showing UV absorbance and radioactivity of organic-extractable pyrene residue in sterile controls (A) and *Mycobacterium* cultures (B) after 96 h of exposure to pyrene.

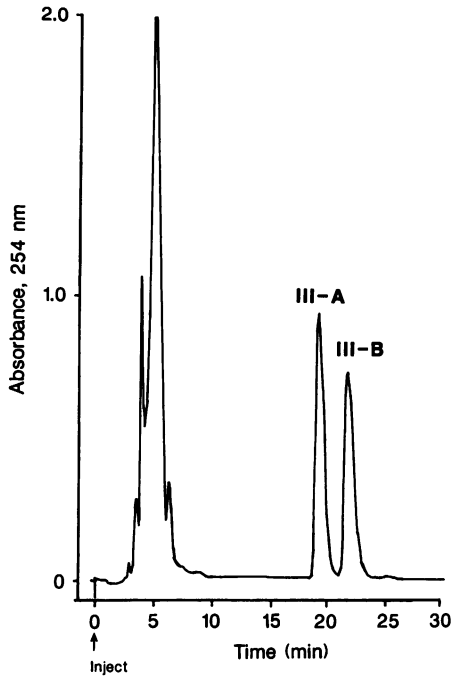

FIG. 2. HPLC elution profile showing the separation of metabolites III-A and III-B on a reversed-phase HPLC system with an isocratic methanol-water (55:45, vol/vol) solvent system.

tion of pyrene, the values in Table 1 are presented as percentages of the remaining organic-extractable ^{14}C-labeled residues and provide a quantitative chemical analysis of nonmineralized pyrene residues at multiple time points.

Undegraded pyrene accounted for over 90% of the organic-extractable residue during the first 24 h of exposure; metabolite levels were quite low, ranging from 0.3 to 3.4%, during the first 18 h of incubation. Pyrene concentrations dropped to 27% at 48 h and further down to 5 to 6% after 72 h. *Mycobacterium* cultures used in this kinetics experiment were pyrene induced, and the initial low accumulation of metabolites occurred during the 18- to 24-h period of highest pyrene mineralization. As pyrene mineralization slowed after 24 h, possibly resulting from loss of cometabolism due to nutrient depletion, an increase in relative concentrations of metabolites was detected. Metabolite II appeared to be the major bacterial metabolite of pyrene, since it occurred at the highest concentration throughout the experiment and accounted for 62.8 to 83.2% of the total organic-extractable ^{14}C-labeled residues during the last 48 h of the experiment. Relative concentrations of metabolites III, IV, and V accounted for 0.9 to 3.3% of the total organic-extractable residue after 48 h. Metabolites III and IV occurred at concentrations of 1.2 to 3.6% during the last 48 h of the experiment, but metabolite V dropped from a high of 2.0% at 48 h down to 0.9% after 96 h. Highly polar metabolites increased from 0.2 to 0.4% early in the experiment to 1.9 to 4.6% during the last 48 h of incubation.

Identification of initial ring-oxidation metabolites. Metabolite III had an HPLC retention time of 16.6 min (Fig. 1) and accounted for 0.4 to 3.6% of the organic extractable ^{14}C-labeled residue (Table 1). This metabolite appeared as a single compound on prep-TLC and gradient reverse-phased HPLC but eluted from isocratic reversed-phase HPLC as two separate compounds. Figure 2 shows the elution profile of the metabolites, designated III-A and III-B, which eluted at 19.2 and 21.8 min, respectively, on the isocratic HPLC system. Repeated injections allowed the isolation and purification of sufficient quantities of III-A and III-B for further structural analyses.

The UV-visible absorption spectra of both III-A and III-B showed absorption maxima at 220, 257, 286 (shoulder), and 298 nm. Figure 3 shows the mass spectra obtained by direct-probe MS analyses of metabolites III-A and III-B. Both metabolites had a M^+ at *m/z* 236, a base peak at *m/z* 218 ($M^+ - 18$, H_2O loss), and fragment ions at *m/z* 189, 176, and 94 which were similar to authentic pyrene *trans*- and *cis*-4,5-dihydrodiols. The patterns of HPLC retention times, UV-visible absorption, and mass spectra suggested that metabolites III-A and III-B were both pyrene dihydrodiols. However, these analyses did not allow us to determine the structures of III-A and III-B.

Thus, NMR analyses were utilized for structural identification of these metabolites. The NMR spectra for III-A and III-B are shown in Fig. 4A and B, respectively. The 500-MHz ^1H spectral assignments of III-A were as follows: (acetone-d_6) 5.07 (s, 2, $H_{4,5}$), 7.65 (dd, 2, $J_{1,2}$ = 7.3 Hz, $J_{2,3}$ = 7.9 Hz, $H_{2,7}$), 7.83 (s, 2, $H_{9,10}$), 7.87 (d, 2, $H_{1,8}$), and 7.90 (d, 2, $H_{3,6}$) ppm. These chemical shifts and coupling patterns were consistent with and identical to the ^1H NMR spectral data of authentic pyrene *trans*-4,5-dihydrodiol. The 500 MHz NMR spectral assignments of III-B were as follows: (acetone-d_6) 5.14 (s, 2, $H_{4,5}$), 7.64 (dd, 2, $J_{1,2}$ = 7.2 Hz, $J_{2,3}$ = 8.6 Hz, $H_{2,7}$), 7.82 (d, 2, $H_{1,8}$), 7.84 (s, 2, $H_{9,10}$), and 7.89 (d, 1, H_3) ppm. These chemical shifts and coupling patterns

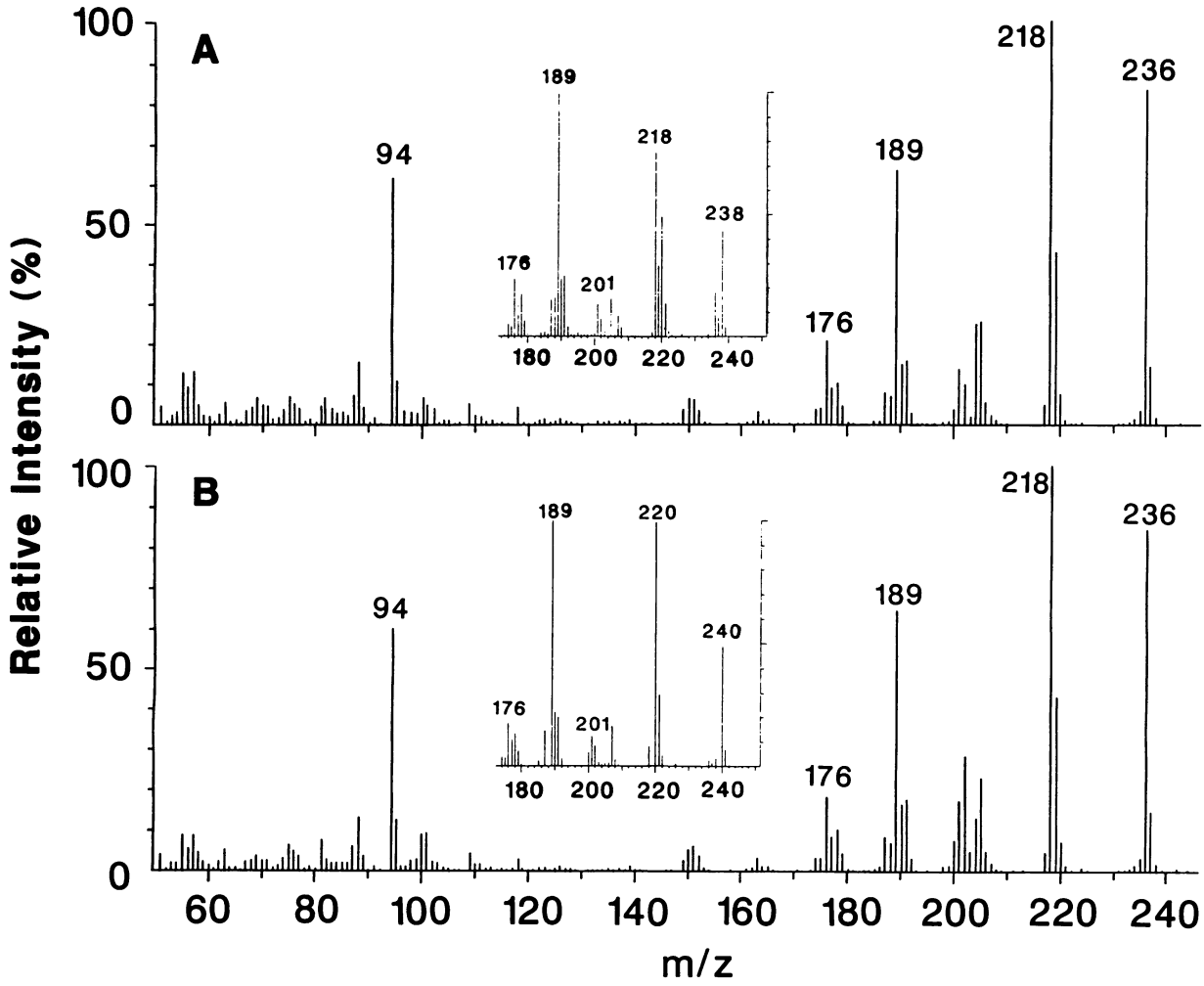

FIG. 3. Mass spectra of pyrenedihydrodiol metabolites III-A (A) and III-B (B). The insets are the mass spectra for the $^{18}O_2$ experiments.

were also consistent with and identical to the ^1H NMR spectral data of authentic pyrene *cis*-4,5-dihydrodiol.

The proton NMR spectra of pyrene dihydrodiols III-A and III-B both exhibit A_2 spin systems and show characteristics for the $H_{4,5}$ resonance which are expected for an A_2 system where $J_{4,5} = 0.0$ or greater (11). There are two differences in the spectral parameters for III-A and III-B. The different chemical shifts for $H_{4,5}$ of 5.07 and 5.14 ppm, respectively, are associated with the proximity of $H_{4,5}$ protons to the neighboring oxygen of the dihydrodiol and are caused by the gouch-associated interactions. The larger and more significant chemical shift difference in the spectral data for III-A and III-B occurs for the $H_{1,8}$ protons. The $H_{1,8}$ proton resonances for the *cis* isomer (III-B) exhibits an upfield shift compared with the $H_{1,8}$ proton resonance of the *trans* isomer (III-A). This difference results from a twisting of the aromatic system to help relieve the gouch interactions between the OH moieties at the 4 and 5 positions. The twisting of the aromatic system of the *cis* isomer forces the $H_{1,8}$ protons to less neighboring ring current effect than the $H_{1,8}$ protons of the *trans* isomer.

Optically active dihydrodiols resulting from stereoselective metabolism of PAHs by rat liver microsomes, bacteria, and fungi have been reported (1, 6, 29). Circular dichroism spectra for pyrene dihydrodiols III-A and III-B were obtained. Metabolite III-A was optically active, and the circular dichroism spectrum showed a negative Cotton effect. Metabolite III-B was not optically active. The assignment of the absolute stereochemistry of pyrene dihydrodiol III-A was not pursued because an authentic pyrene dihydrodiol standard of known enantiomeric purity was not available for comparison. However, differences observed in optical activity did provide some information regarding differences between pyrene dihydrodiols III-A and III-B. For example, an optically inactive pyrene dihydrodiol is either a racemic mixture of enantiomers resulting from nonstereoselective metabolism or, in the case of pyrene *cis*-4,5-dihydrodiol, is a *meso* compound (a molecule which can be superimposed on its mirror image even though it contains asymmetric carbon atoms). These data suggest that optically inactive pyrenedihydrodiol III-B must be either a racemic mixture of enantiomers or a pyrene *cis*-4,5-dihydrodiol. Furthermore, this reasoning would suggest that optically active pyrene dihydrodiol III-A is a nonracemic *trans* isomer and cannot be pyrene *cis*-4,5-dihydrodiol.

The assignments of pyrene *trans*- and *cis*-4,5-dihydrodiol for metabolites III-A and III-B, respectively, were supported by the UV spectra and HPLC and GC-MS retention times for authentic pyrene *trans*- and *cis*-4,5-dihydrodiols. The UV spectra of authentic standards were identical to

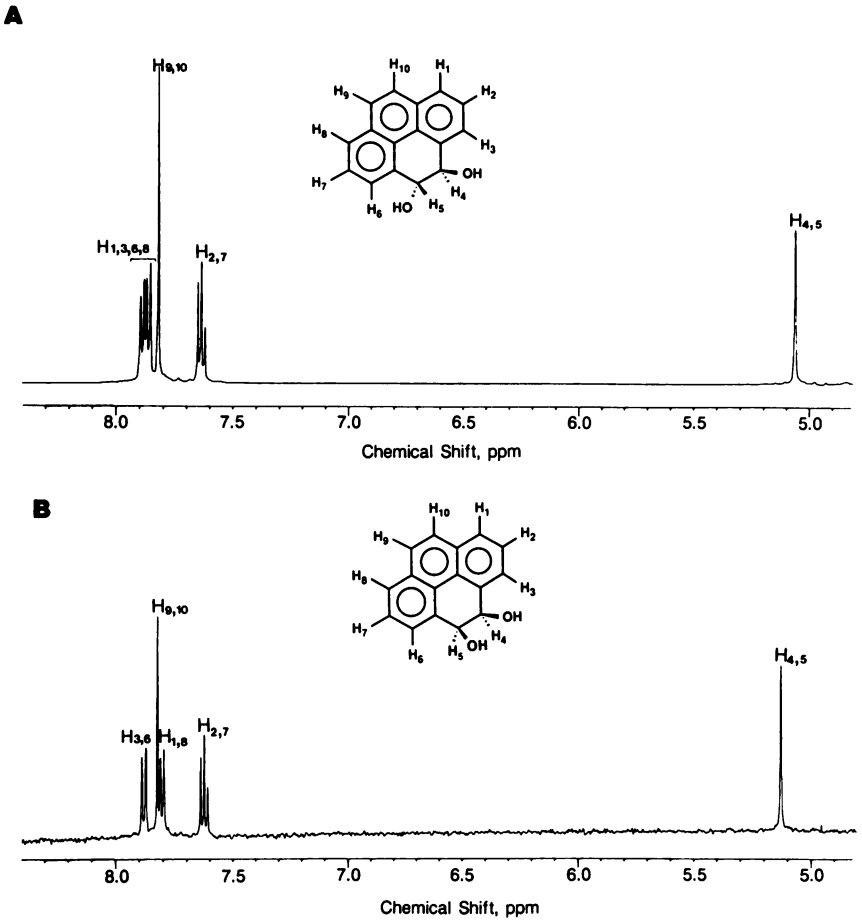

FIG. 4. Proton NMR spectra (500 MHz) for pyrenedihydrodiol metabolites III-A (A) and III-B (B) formed from pyrene by a *Mycobacterium* sp.

those of metabolites III-A and III-B (data not shown). Furthermore, HPLC analyses with the isocratic (methanol-water, 55:45) solvent system showed that authentic *trans*- and *cis*-pyrenedihydrodiols were separated and had retention times of 19.2 and 21.8 min, respectively, which were identical to those of metabolites III-A and III-B, respectively (Fig. 2). Similarly, capillary column GC-MS analyses showed a 6-s separation of diacetylated authentic pyrene *trans*- and *cis*-4,5-dihydrodiols. Authentic pyrene *trans*-4,5-dihydrodiol and III-A had identical retention times of 14 min and 2 s, whereas authentic pyrene *cis*-4,5-dihydrodiol and III-B had identical retention times of 14 min and 8 s (data not shown).

Metabolite IV occurred at a lower concentration (0.5 to 1.7%) than the other metabolites and appeared to peak in concentration after 48 h of incubation (Table 1). Metabolite IV had an HPLC retention time of 22.0 min, which would be characteristic of a pyrene ring oxidation product. Repeated attempts to isolate and purify sufficient quantities of metabolite IV for further chemical analyses were unsuccessful, and the identity of this metabolite is not known. There were some indications that metabolite IV may be chemically unstable. The decrease in concentration of metabolite IV late in the experiment suggests that it was utilized as chemical substrate for further enzymatic reactions.

Metabolite V had an HPLC retention time of 26 min (Fig. 1) and accounted for 0.2 to 2.0% of the organic-extractable residue throughout the experiment (Table 1). Acetylation of the extract and analysis by capillary column GC-MS showed a metabolite with a GC-MS retention time of 10.45 min. MS analysis of derivatized metabolite V (Fig. 5) gave a molecular ion (M^+) at *m/z* 260, a base peak at *m/z* 218 ($M^+ - 42$, O=C=CH_2 loss), and a fragment ion at *m/z* 189 (further —CHO loss). The HPLC and GC-MS retention times and the MS fragmentation pattern were identical to those of acetylated authentic 1-hydroxypyrene. However, the position of the hydroxyl substituent on the pyrene ring could not be determined, since an amount sufficient for NMR analyses was not obtained.

Identification of ring-fission metabolites. Metabolite I had an HPLC retention time of 5.2 min (Fig. 1) and accounted for 0.2 to 5.5% of the organic-extractable residues throughout the experiment. Metabolite I was purified by prep-TLC and isocratic reversed-phase HPLC and was analyzed by UV-visible spectrophotometry and direct-probe MS. The UV-visible absorption spectrum of metabolite I showed absorption maxima at 208, 216, 274, and 319 nm. Metabolite I had an M^+ at *m/z* 196 and fragment ions at *m/z* 168 ($M^+ - 28$) and *m/z* 139 ($M^+ - 57$), which indicate losses of —CO and —CO plus —COH, respectively. This MS analysis of metabolite I is consistent with a molecular formula of $C_{13}H_8O_2$ and an aromatic hydrocarbon containing single keto and hydroxy moieties. Further structural analyses by NMR and IR spec-

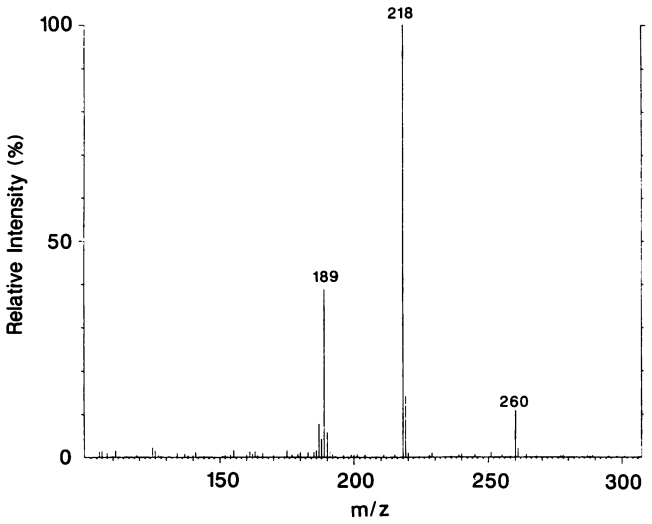

FIG. 5. Mass spectrum of an acetylated derivative of pyrenol (metabolite V) extracted from *Mycobacterium* cultures exposed to pyrene, purified by prep-TLC, and analyzed by capillary column GC-MS (10.45-min retention time).

trometry were conducted to determine the identity of metabolite I.

The 500-MHz ^1H NMR spectrum of metabolite I is shown in Fig. 7. The proton NMR spectral parameters obtained in acetone-d_6 were: 6.53 (d, 1, $J_{1,2}$ of 9.5 Hz, H_2), 7.70 (d, 1, $J_{5,6}$ of 8.6 Hz, H_5), 7.73 (m, 1, H_8), 7.83 (d, 1, H_6), 8.03 (m, 1, H_7 or H_9), 8.13 (d, 1, H_1), and 8.46 (m, 1, H_9 or H_7) ppm. Two coupled vinyl proton doublets were observed at 6.53 (H_2) and 8.13 (H_1) ppm which were consistent with the C=C stretch observed in the IR spectrum at 1,610 cm^{-1} (indicative of a conjugated C=C stretch) and the =C—H in-plane bend observed at 1,405 cm^{-1} in the IR spectrum (24). In addition, the IR spectrum showed an absorption peak at 1,630 cm^{-1}, which is consistent with a conjugated carbonyl moiety. The inability to detect a broad peak for the OH stretch of the phenolic moiety is consistent with weak O—H bonds, which result from tautomerization (24). The remainder of the aromatic resonances observed by NMR were consistent with the chemical shifts and coupling pattern which could be expected for 4-position hydroxyl substitution of perinaphthenone. The chromatographic characteristics, molecular weight, mass spectral fragmentation pattern, and NMR and IR spectra indicated that metabolite I formed from pyrene by a *Mycobacterium* sp. was 4-hydroxyperinaphthenone.

Metabolite II had an HPLC retention time of 7.5 min in the methanol-water solvent system (linear gradient, Fig. 1) and was the major metabolite of pyrene. Metabolite II accounted for 62.8 to 83.2% of the organic-extractable residues after 48 h. This metabolite remained near the origin during prep-TLC with benzene-hexane (1:1, vol/vol) and hexane-acetone (8:2, vol/vol) but had an R_f of 0.35 with a benzene-acetone-acetic acid (85:15:5, vol/vol/vol) solvent system. Metabolite II eluted as a broad peak on reversed-phase HPLC. However, when 1% acetic acid was added to HPLC solvents, the HPLC retention time more than doubled and metabolite II eluted as a single sharp peak (data not shown). The prep-TLC and HPLC chromatographic characteristics observed with metabolite II in the acidic solvent systems are characteristic of a metabolite that is acidic in nature. Repeated injections of metabolite II on an isocratic, acidic reversed-phase HPLC system resulted in the isolation and purification of sufficient quantities for further chemical analyses.

The UV-visible absorption spectrum of metabolite II showed absorption maxima at 212, 254, 276 (shoulder), 285, and 297 nm. Direct-probe MS analysis of metabolite II produced the mass spectrum shown in Fig. 8A. Metabolite II had an M^+ at *m/z* 222 and major fragment ions at *m/z* 205 ($M^+ - 17$) and *m/z* 177 ($M^+ - 45$) representing probable losses of —OH and —COOH, respectively, which are characteristic of organic acids. Fragment ions were also observed at m/z 194 ($M^+ - 28$), possibly due to $CH_2{=}CH_2$ loss from an aromatic ring and at *m/z* 165 (*m/z* 177 to 12, loss of —C) and *m/z* 151 ($M^+ - 71$) possibly due to loss of —CHCCOOH plus H from an accompanying hydrogen shift.

The 500-MHz ^1H NMR spectrum in a mixture of methanol-d_4 and deuterium oxide for metabolite II shown in Fig. 9 is consistent with 4-phenanthroic acid. The NMR spectral parameters obtained from metabolite II were as follows: 7.62 (dd, 1, $J_{5,6}$ of 8.2 Hz, H_6), 7.66 (dd, 1, $J_{7,8}$ of 7.7 Hz, H_7), 7.67 (dd, 1, $J_{1,2}$ of 7.3 Hz, $J_{2,3}$ of 7.7 Hz, H_2), 7.71 (d, 1, H_1), 7.81 to 7.87 (m_{AB}, 2, $J_{9,10}$ of 9.0 Hz, H_9, H_{10}), 7.98 (d, 1, H_8), 8.03 (d, 1, H_3), and 8.62 (d, 1, H_5) ppm. The presence of only one downfield resonance peak at 8.62 ppm indicates that there is only one aromatic proton at the bay region and thus indicates that the COOH functional group is located at the C-4 position. The protons at positions 9 and 10 are typical K-region AB spin systems (7.81 to 7.87 ppm) with a 9.0-Hz coupling. The coupling pattern and chemical shifts exhibited by H_1, H_2, and H_3 (7.71, 7.67, and 8.03 ppm, respectively) were characteristic of coupling patterns and chemical shift positions (relative to the H_5 bay-region proton) expected of 4-position substitution of phenanthrene. The anisotropic effects and loss of conjugative effect of the carbonyl system caused the H_3 and H_5 protons not to be shifted downfield as far as might be expected for a fully planar carbonyl moiety.

A portion of metabolite II was derivatized with diazomethane and analyzed by capillary column GC-MS. The methylated derivative of metabolite II had a capillary column GC retention time of 12.5 min and produced the spectrum shown in Fig. 8B. An M^+ was observed at *m/z* 236, representing a 14-mass-unit increase over underivatized metabolite II (Fig. 8A), which is characteristic of single methylation of an organic acid. Fragment ions observed at *m/z* 221 ($M^+ - 15$, loss of —CH_3) and *m/z* 205 ($M^+ - 31$, loss of —OCH_3) show a fragmentation pattern indicative of a monomethylated organic acid. Fragment ions observed at *m/z* 177 ($M^+ - 59$, loss of —$COOCH_3$), *m/z* 165, and *m/z* 151 were similar to those observed for underivatized metabolite II (Fig. 8A).

The structural assignment for 4-phenanthroic acid was further substantiated by the IR spectrum of a methylated derivative of metabolite I, which showed a strong carbonyl

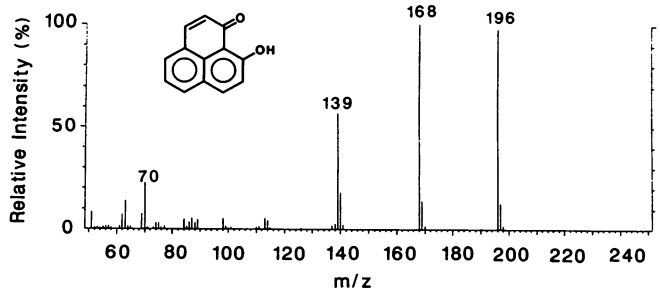

FIG. 6. Mass spectrum of metabolite I formed from pyrene by a *Mycobacterium* sp.

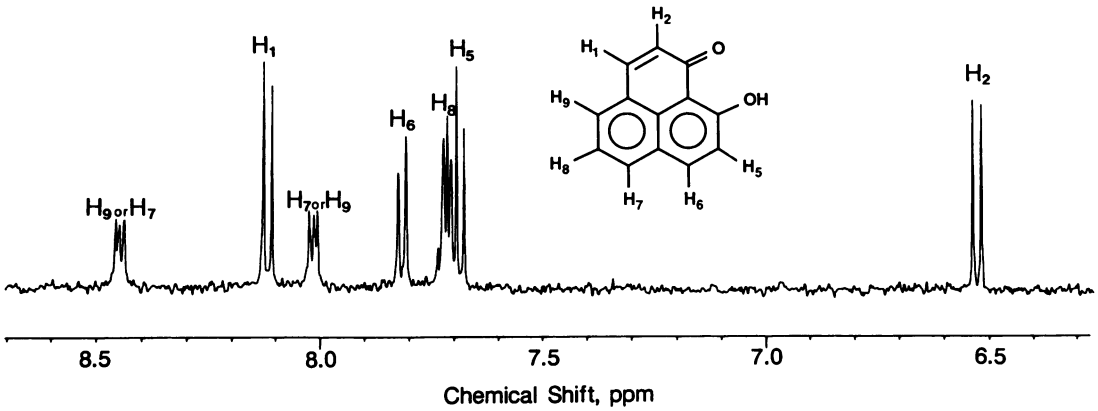

FIG. 7. The 500-MHz NMR spectrum for 4-hydroxyperinaphthenone (metabolite I).

stretch at 1,730 cm^{-1}, which is indicative of a methyl ester of an aromatic acid, and a strong carbon-carbon double bond stretch (C=C) at 1,460 cm^{-1}, which is typical for highly aromatic ring systems. The chromatographic characteristics, molecular weight, single methylation, MS fragmentation patterns, and NMR and IR spectra observed for metabolite II indicated that it was 4-phenanthroic acid.

Highly polar metabolites of pyrene were not retained on reversed-phase HPLC and accounted for 0.2 to 1.9% of the total extractable ^{14}C residue during the first 48 h of exposure but increased to 4.5% after 96 h of exposure. These polar residues were further purified with TLC and a silica gel Sep-Pak. Pooled polar ^{14}C residues were methylated with diazomethane, acetylated with acetic anhydride, and analyzed by capillary column GC-MS. Figure 10A shows the spectrum for a derivatized polar metabolite that had a GC-MS retention time of 9 min and 42 s. This derivatized metabolite had an M^+ at *m/z* 194 and fragmentation ions at *m/z* 163 ($M^+ - 31$, —OCH_3 loss) and *m/z* 133 ($M^+ - 61$, —OCH_3 and —OCH_2 losses). The ion observed at *m/z* 154 is from a coeluting contaminant. The GC-MS retention time and MS fragmentation pattern for this derivatized polar metabolite were identical to those of a dimethylated standard of phthalic acid. A second polar metabolite was detected which had a GC-MS retention time of 10 min and 16 s (Fig. 10B). This derivatized metabolite had an M^+ at *m/z* 162 and fragmentation ions at *m/z* 131 ($M^+ - 31$, —OCH_3 loss) and at *m/z* 91, which probably resulted from rearrangement to a tropylium ion (C_7H_7). The GC-MS retention time and MS fragmentation pattern for this derivatized polar metabolite were identical to those of a methylated standard of cinnamic acid.

Monooxygenase- and dioxygenase-mediated oxidation of pyrene. The enzymatic hydroxylation of PAHs may be catalyzed by monooxygenase and dioxygenase enzymes involving the single or double insertion, respectively, of atoms from molecular oxygen into the aromatic nucleus. Monooxygenase- and dioxygenase-mediated reactions may be distinguished by incubating cultures in an $^{18}O_2$ atmosphere and measuring either single or double oxygen insertions into the aromatic rings (12). For example, a single oxygen insertion (monooxygenase) in the presence of $^{18}O_2$ will produce a 2-unit mass increase in the molecular weight of the product, whereas a double oxygen insertion (dioxygenase) will result in a 4-unit mass increase. *Mycobacterium* cultures were exposed to pyrene in a $^{18}O_2$ atmosphere for 48 h, and the pyrene *cis*- and *trans*-4,5-dihydrodiols were extracted and purified as described above.

MS analyses of the headspace gas in the closed flasks showed that the relative percentage of $^{18}O_2$ was 96.8 ± 0.5% at 0 h and 95.5 ± 0.6% after 48 h. Figure 3 (insets) shows the mass spectra for pyrene *trans*- and *cis*-4,5-dihydrodiols (III-A and III-B, respectively) produced by the mycobacterium in the $^{18}O_2$ atmosphere. The pyrene *trans*-4,5-dihydrodiol had an M^+ at *m/z* 238 which is a 2-mass-unit increase over the M^+ of *m/z* 236 observed for pyrenedihydrodiols in a $^{16}O_2$ atmosphere (Fig. 3A, inset) and is characteristic of monooxygenase-catalyzed hydroxylation of pyrene. The pyrene *cis*-4,5-dihydrodiol produced by the *Mycobacterium* had an M^+ at *m/z* 240 (Fig. 3B, inset), a 4-mass-unit increase characteristic of dioxygenase-catalyzed hydroxylation of pyrene. Fragment ions observed for both pyrene *trans*- and *cis*-dihydrodiols at *m/z* 189, 176, and 94 were identical to those of authentic pyrenedihydrodiol standards. In addition, the pyrene *cis*-dihydrodiol spectra contained an *m/z* 220 ion that is consistent with $^{18}O_2$ incorporation in the molecule ($M^+ - H_2O$). The monoincorporated dihydrodiol (M^+, *m/z* 238) showed a significant water loss fragment to form *m/z* 218.

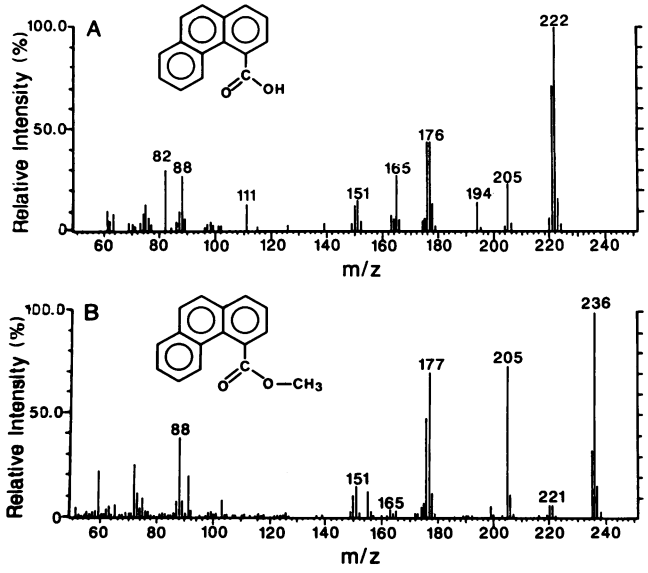

FIG. 8. Mass spectra of unmethylated (A) and methylated (B) 4-phenanthroic acid (metabolite II), the major product formed from pyrene by the *Mycobacterium* sp.

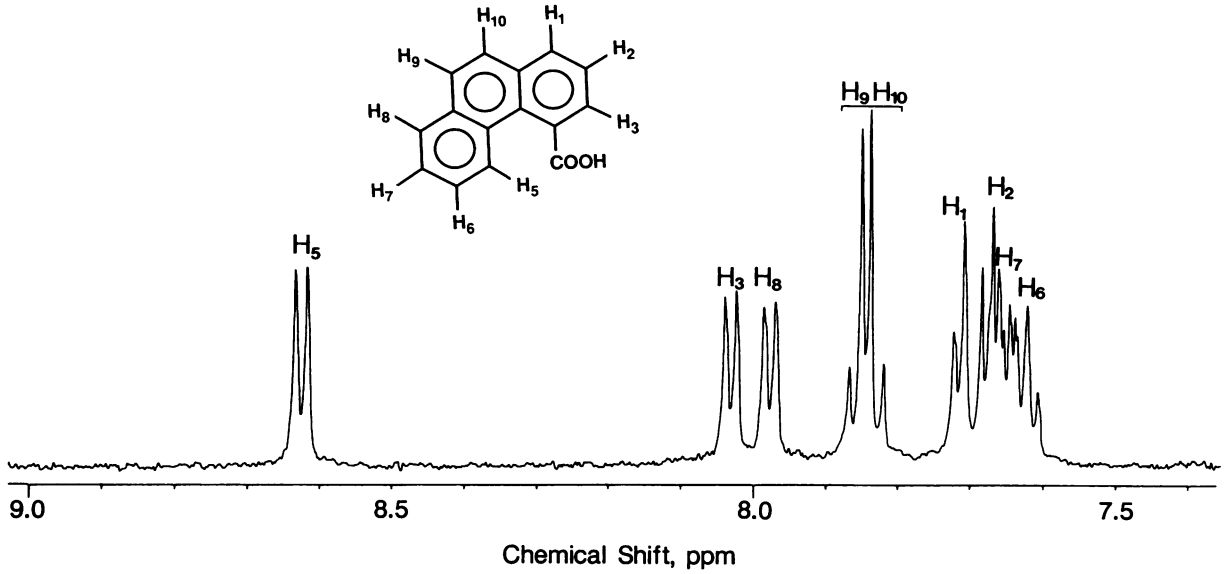

FIG. 9. The 500-MHz NMR spectrum for metabolite II (4-phenanthroic acid).

DISCUSSION

The PAH-degrading *Mycobacterium* sp. used in this study was recently isolated from an ecosystem chronically exposed to petrogenic hydrocarbons (13–16). We previously reported mineralization of naphthalene, phenanthrene, pyrene, 1-nitropyrene, fluoranthene, 6-nitrochrysene, and 3-methylcholanthrene by this *Mycobacterium* sp. (14). Furthermore, this *Mycobacterium* sp. mineralized four-ringed PAHs faster than two- or three-ringed PAHs. In the present study, the *Mycobacterium* sp. was used to study the microbial metabolism of pyrene, a PAH containing four aromatic rings. This is the first report on the enzymatic mechanisms and identification of ring oxidation and fission products for the microbial metabolism of pyrene (Fig. 11). Although pyrene is not genotoxic, it has a four-ringed aromatic nucleus which is found in several carcinogenic PAHs such as benzo[*a*]pyrene, indeno(1,2,3-*cd*) pyrene, and 1-nitropyrene. The initial oxidative attack on pyrene by the mycobacterium resulted in the formation of dihydrodiols at the 4,5 position (K region). Procaryotes are known to utilize dioxygenase enzymes to insert both atoms of molecular oxygen into aromatic hydrocarbons to form dihydrodiols with a *cis* configuration (Cerniglia and Heitkamp, in press). However, the formation of both *cis*- and *trans*-4,5-dihydrodiols of pyrene by the *Mycobacterium* sp. in this study suggested

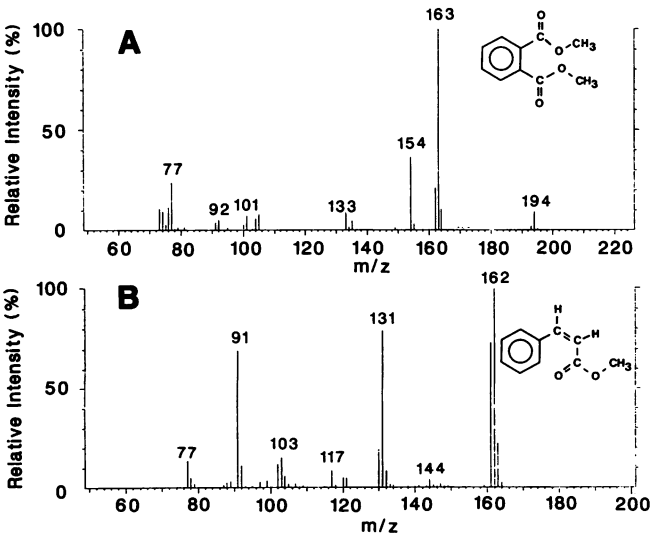

FIG. 10. Mass spectra of derivatized polar metabolites analyzed by GC-MS with retention times of 9 min and 42 s (A) and 10 min and 16 s (B).

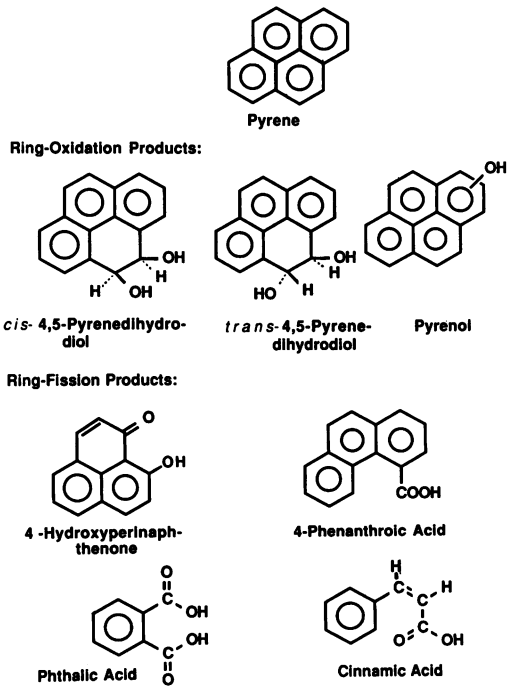

FIG. 11. Structures of identified pyrene metabolites produced by the *Mycobacterium* sp.

multiple pathways for the initial oxidative attack on pyrene. This was confirmed by the experiments with $^{18}O_2$, which showed that pyrene *cis*-dihydrodiol formation was a dioxygenase-catalyzed reaction and that pyrene *trans*-dihydrodiol formation was catalyzed by monooxygenase enzymes. The involvement of a specific monooxygenase for the epoxidation of short-chain alkenes has been reported for a *Mycobacterium* sp. (8). It is believed that *cis*-dihydrodiols undergo rearomatization to hydroquinone derivatives, which are precursors for ring cleavage and further metabolism (Cerniglia and Heitkamp, in press). This is supported by the relative differences observed between the concentrations of pyrene *cis*- and *trans*-dihydrodiols in this study (data not shown). The concentration of pyrene *trans*-dihydrodiol peaked after about 48 h, and levels persisted throughout the experiment. In contrast, pyrene *cis*-dihydrodiol concentrations peaked at levels similar to those of the *trans* isomer after 48 h but then disappeared after 72 h of incubation. Presumably, the disappearance of pyrene *cis*-dihydrodiol resulted from further microbial metabolism to ring fission products.

Mammalian metabolism of pyrene results in the formation of *trans*-4,5-pyrenedihydrodiol, 1-hydroxypyrene, pyrenediphenols, and quinones, which may be eliminated directly or undergo secondary metabolism to form highly water-soluble glucuronide, sulfate, or glutathione conjugates (19). Many eucaryotic microorganisms contain monooxygenase enzyme systems that mimic several of the chemical biotransformations observed in mammals (27, 28). Recently, Cerniglia et al. (5) reported that *Cunninghamella elegans* metabolized pyrene to phenolic derivatives, which underwent secondary metabolism to form glucoside conjugates. In addition, two pyrenequinones were formed which may be of toxicological significance, since they have been shown to enhance the mutagenicity of other toxicants (25). Although pyrene *trans*-4,5-dihydrodiol occurs as a major product of monooxygenases in mammals, it was not detected as a fungal metabolite of pyrene.

The pyrene *trans*-4,5-dihydrodiol produced by the *Mycobacterium* sp. in this study is the first reported monooxygenase-catalyzed *trans*-dihydrodiol formed from a PAH by a bacterium. In most microorganisms, monooxygenase activities have been attributed to cytochrome P-450-dependent enzyme systems (27, 28). However, the existence of other microbial cytochromes and oxygenase enzyme systems has also been reported (2, 30). DeBont and co-workers (8) have reported a specific monooxygenase in *Mycobacterium* sp. strain E20 involved in the epoxidation of short-chain alkenes. The detection and characterization of a possible cytochrome P-450-dependent monooxygenase enzyme system in this pyrene-degrading *Mycobacterium* sp. warrants further investigation.

Pyrenol was detected as an initial ring oxidation product of pyrene produced by the mycobacterium, but an amount sufficient for further structural analyses was not obtained and the ring position for the hydroxyl moiety is not known. 1-Hydroxypyrene has been reported as the major metabolite of pyrene occurring in the urine of pigs exposed orally to pyrene (20). In addition, 1-hydroxypyrene has been reported as a fungal metabolite of pyrene (5). It is unclear whether the small amounts of pyrenol in the present study occurred from nonenzymatic dehydration of pyrene dihydrodiols or from oxidative metabolism of pyrene by the mycobacterium.

Clearly, most of the organic-extractable residues after 48 h of incubation with the mycobacterium were highly polar ring oxidation products. The major metabolite of pyrene produced by the mycobacterium was 4-phenanthroic acid. Interest in the chemical properties of 4-phenanthroic acid as a model chemical for molecular overcrowding due to bay-region substitution has existed since a method for the organic synthesis of 4-phenanthroic acid was reported by Rutherford and Newman (26). However, the present study is the first report of 4-phenanthroic acid as a bacterial metabolite of PAHs. 4-Phenanthroic acid probably occurs as a ring fission product of *cis*-4,5-pyrenedihydrodiol, but the mechanism of this 1-carbon excision from the K region of pyrene is not known. Observed concentrations of the *cis* isomer of pyrenedihydrodiol relative to the *trans* isomer decreased late in the study, which would support the conclusion that the *cis* isomer was further metabolized to 4-phenanthroic acid and other metabolites. Since similar K-region attack and 1-carbon excisions by bacteria have not been previously reported for other PAHs, the chemical pathway for the degradation of other PAHs containing K regions by this mycobacterium warrants investigation.

Although pyrene 1,2-dihydrodiol was not detected as a ring oxidation metabolite of pyrene in this study, the clustered, 13-carbon, three-ringed structure of 4-hydroxyperinaphthenone (Fig. 11) probably resulted from ring oxidation and cleavage of the alpha ring of pyrene. The lack of accumulation of a 1,2-pyrenedihydrodiol does not preclude it as an intermediate in the formation of 4-hydroxyperinaphthenone but may only indicate that the ring fission reactions occur quickly once the alpha ring is oxidized. The 4-hydroxyperinaphthenone described in this study has a novel chemical structure, and its IR characteristics and UV, MS, and NMR spectra have not previously been reported.

Cinnamic acid and phthalic acid were also detected as highly polar metabolites of pyrene in this study. However, it is unclear whether these metabolites resulted from further metabolism of 4-phenanthroic acid, 4-hydroxyperinaphthenone, or other chemical intermediates. The origin of these polar, single-ringed metabolites may be resolved in future studies in which large quantities of each ring fission intermediate are synthesized and utilized as substrate for microbial metabolism.

The degradability of the ring fission products of pyrene identified in this study may be an important factor affecting the enhancement of biodegradation of high-molecular-weight PAHs in the environment. For example, Herbes and Schwall (17) reported a lack of accumulated intermediates from the degradation of PAHs in sediments. A similar lack of chemical intermediates was observed for the degradation of PAHs containing three or more aromatic rings in sediment-water microcosms in the present study. These findings are consistent with the hypothesis that the rate-limiting step for the biodegradation of PAHs may be the initial ring oxidation reaction, after which degradation by natural mixed bacterial cultures proceeds relatively quickly with little or no accumulation of intermediates. If this is true, PAH-oxidizing bacteria inoculated into PAH-contaminated sites may enhance degradation by producing ring oxidation or fission products which may be readily degraded by indigenous microorganisms.

In the accompanying paper (15), we indicated that inducible enzymes appear to be responsible for pyrene catabolism in this mycobacterium since lag phases in pyrene mineralization were observed in cultures grown in the absence of pyrene and no pyrene mineralization was observed in non-induced cultures dosed with chloramphenicol. Inducible pyrene-degrading enzymes in this mycobacterium may be either chromosome or plasmid mediated. Crawford and

Bates (7) have isolated plasmid DNA from several strains of *Mycobacterium avium-M. intracellulare*. However, initial studies to isolate and identify plasmids in this *Mycobacterium* sp. were not successful because of very high activities of nuclease enzymes, which degraded the bacterial DNA during processing. The isolation and identification of a pyrene-degrading plasmid in this *Mycobacterium* sp. may have practical application for future cloning studies to construct genetically engineered bacteria able to degrade PAHs. The inducibility of pyrene-degrading enzymes in this mycobacterium is consistent with the observed inducibility of hydrocarbon-degrading enzymes encoded on plasmids containing both structural and regulatory genes in other bacteria (31).

ACKNOWLEDGMENTS

We thank David T. Gibson and Peter P. Fu for helpful discussions and reviewing the manuscript. We also thank Rebecca Robertson for technical assistance and LaTonya Williams for typing the manuscript.

LITERATURE CITED

1. **Akhtar, M. N., D. R. Boyd, N. J. Thompson, M. Koreeda, D. T. Gibson, V. Mahadevan, and D. M. Jerina.** 1975. Absolute stereochemistry of the dihydroanthracene-*cis*- and *trans*-1,2-diols produced from anthracene by mammals and bacteria. J. Chem. Soc. **23**:2506–2511.
2. **Bernhardt, F. H., H. Pachowsky, and H. Staudinger.** 1975. A 4-methoxybenzoate *O*-demethylase from *Pseudomonas putida*—a new type of monooxygenase system. Eur. J. Biochem. **57**:241–256.
3. **Cerniglia, C. E.** 1984. Microbial metabolism of polycyclic aromatic hydrocarbons. Adv. Appl. Microbiol. **30**:31–71.
4. **Cerniglia, C. E., J. P. Freeman, and R. K. Mitchum.** 1982. Glucuronide and sulfate conjugation in the fungal metabolism of aromatic hydrocarbons. Appl. Environ. Microbiol. **43**:1070–1075.
5. **Cerniglia, C. E., D. W. Kelly, J. P. Freeman, and D. W. Miller.** 1986. Microbial metabolism of pyrene. Chem. Biol. Interact. **57**: 203–216.
6. **Cerniglia, C. E., and S. K. Yang.** 1984. Stereoselective metabolism of anthracene and phenanthrene by the fungus *Cunninghamella elegans*. Appl. Environ. Microbiol. **47**:119–124.
7. **Crawford, J. T., and J. H. Bates.** 1979. Isolation of plasmids from *Mycobacteria*. Infect. Immun. **24**:979–981.
8. **DeBont, J. A. M., M. M. Attwood, S. B. Primrose, and W. Harder.** 1979. Epoxidation of short chain alkenes in *Mycobacterium* E20: the involvement of a specific monooxygenase. FEMS Microbiol. Lett. **6**:183–188.
9. **Gibson, D. T., V. Mahadevan, D. M. Jerina, H. Yagi, and H. J. C. Yeh.** 1975. Oxidation of the carcinogens benzo[a]pyrene and benz[a]anthracene to dihydrodiols by a bacterium. Science **189**:295–297.
10. **Gibson, D. T., and V. Subramanian.** 1984. Microbial degradation of aromatic hydrocarbons, p. 181–252. *In* D. T. Gibson (ed.), Microbial degradation of organic compounds. Marcel Dekker, Inc., New York.
11. **Gunther, H.** 1980. NMR spectroscopy, p. 436. (Translated by R. W. Gleason.) John Wiley & Sons, Inc., New York.
12. **Hayaishi, O.** 1966. Enzymatic studies on the mechanism of double hydroxylation. Pharmacol. Rev. **18**:71–75.
13. **Heitkamp, M. A., and C. E. Cerniglia.** 1987. Effects of chemical structure and exposure on the microbial degradation of polycyclic aromatic hydrocarbons in freshwater and estuarine ecosystems. Environ. Toxicol. Chem. **6**:535–546.
14. **Heitkamp, M. A., and C. E. Cerniglia.** 1988. Mineralization of polycyclic aromatic hydrocarbons by a bacterium isolated from sediment below an oil field. Appl. Environ. Microbiol. **54**:1612–1614.
15. **Heitkamp, M. A., W. Franklin, and C. E. Cerniglia.** 1988. Microbial metabolism of polycyclic aromatic hydrocarbons: isolation and characterization of a pyrene-degrading bacterium. Appl. Environ. Microbiol. **54**:2549–2555.
16. **Heitkamp, M. A., J. P. Freeman, and C. E. Cerniglia.** 1987. Naphthalene biodegradation in environmental microcosms: estimates of degradation rates and characterization of metabolites. Appl. Environ. Microbiol. **53**:129–136.
17. **Herbes, S. E., and L. R. Schwall.** 1978. Microbial transformation of polycyclic aromatic hydrocarbons in pristine and petroleum-contaminated sediments. Appl. Environ. Microbiol. **35**:306–316.
18. **Holder, C. L., W. A. Korfmacher, W. Slikker, H. C. Thompson, and A. B. Gosnell.** 1985. Mass spectral characterization of doxylamine and its Rhesus monkey urinary metabolites. Biomed. Mass Spectrom. **12**:151–158.
19. **Jacob, J., G. Grimmer, G. Raab, and A. Schmoldt.** 1982. The metabolism of pyrene by rat liver microsomes and the influence of various mono-oxygenase inducers. Xenobiotica **12**:45–53.
20. **Keimig, S. D., K. W. Kirby, and D. P. Morgan.** 1983. Identification of 1-hydroxypyrene as a major metabolite of pyrene in pig urine. Xenobiotica **13**:415–420.
21. **Keith, L. H., and W. A. Telliard.** 1979. Priority pollutants I—a perspective view. Environ. Sci. Technol. **13**:416–423.
22. **Miller, E. C., and J. A. Miller.** 1981. Searches for ultimate chemical carcinogens and their reactions with cellular macromolecules. Cancer **47**:2327–2345.
23. **Mortelmans, K., S. Haworth, T. Lawlor, W. Speck, B. Tainer, and E. Zeiger.** 1986. Salmonella mutagenicity tests. II. Results from the testing of 270 chemicals. Environ. Mutagen. **8**(Suppl. 7):1–119.
24. **Nakanishi, K., and P. H. Solomon.** 1977. Infrared absorption spectroscopy, p. 25. Holden-Day Inc., San Francisco.
25. **Okamoto, H., and D. Yoshida.** 1981. Metabolic formation of pyrenequinones as enhancing agents of mutagenicity in *Salmonella*. Cancer Lett. **11**:215.
26. **Rutherford, K. G., and M. S. Newman.** 1957. A new synthesis and some reactions of 4-phenanthrenecarboxylic acid. J. Am. Chem. Soc. **79**:213–214.
27. **Smith, R. V., D. Acosta, and J. P. Rosazza.** 1977. Cellular and microbial models in the investigation of mammalian metabolism of xenobiotics. Adv. Biochem. Eng. **5**:69–100.
28. **Smith, R. V., and P. J. Davis.** 1980. Induction of xenobiotic monooxygenases. Adv. Biochem. Eng. **14**:61–100.
29. **Von Tungeln, L. S., and P. P. Fu.** 1986. Stereoselective metabolism of 9-methyl, 9-hydroxymethyl and 9,10-dimethylanthracenes: absolute configurations and optical purities of *trans*-dihydrodiol metabolites. Carcinogenesis **7**:1135–1141.
30. **Webster, D. A., and D. P. Hackett.** 1966. The purification and properties of cytochrome o from *Vitreoscilla*. J. Biol. Chem. **241**:3308–3315.
31. **Williams, P. A.** 1981. Genetics of biodegradation, p. 97–130. *In* T. Leisinger, R. Hutter, A. M. Cook, and J. Nuesch (ed.), Microbial degradation of xenobiotics and recalcitrant compounds. Academic Press, Inc., New York.